Temperature-dependent screening and carrier-carrier scattering in heavily doped semiconductors

Kjeld O. Jensen
Department of Physics, University of Essex, Colchester CO4 3SQ, United Kingdom

J. M Rorison
Sharp Laboratories of Europe Ltd., Oxford OX4 4GA, United Kingdom

Alison B. Walker
School of Physics, University of East Anglia, Norwich NR4 7TJ, United Kingdom
(Received 9 November 1992; revised manuscript received 18 May 1993)

We present an analysis of the scattering of hot carriers by conduction electrons in heavily doped semiconductors within the random-phase approximation (RPA). Different approximations to the temperature-dependent RPA are considered: (i) the two-pole approximation developed by Rorison and Herbert, (ii) the plasmon-pole approximation, and (iii) the Lindhard dielectric function. We present a range of results for n-doped GaAs for different carrier energies, doping levels, and temperatures, and we examine the ranges of validity of the different approximations. As an extension of our theory we include, within the two-pole approximation, the coupling of optical phonons to the electron system.

I. INTRODUCTION

In heavily doped semiconductors or semiconductors subject to intense photoexcitation carrier-carrier interactions (electron-electron, hole-hole, and/or electron-hole) become very important. In the analysis of transport in hot-electron transistors/spectrometers[1] and heterojunction bipolar transistors[2] scattering by carriers and polar longitudinal-optical (LO) phonons are found to be the dominant scattering mechanism for hot carriers. It is therefore necessary to have a good knowledge of the details of the carrier-carrier and carrier-phonon interactions and their interplay.

The analysis of the interactions between a carrier and a medium involves the study of the frequency (ω) and wave-vector (q) -dependent dynamical screening function $\epsilon(\omega, q)$. For heavily doped semiconductors and metals the random-phase approximation (RPA) provides an accurate description.[3,4] Most of the various treatments of carrier-carrier interaction involve this approximation. For high carrier density systems such as metals, the zero-temperature RPA works well with $\epsilon(\omega, q)$ being the Lindhard dielectric function.[5,6] In this regime it is possible to make a clear distinction between collective (plasmon) and single-particle excitations and one can with reasonable accuracy divide the carrier-carrier interaction into collective and single-particle parts through the introduction of a cutoff wave vector.[7,8] However, for the lower carrier densities and lower excitation energies found in doped or optically excited semiconductors temperature effects are significantly more important than for metals. A result of this is that the collective and single-particle excitation modes become intricately coupled, making separation of these modes very difficult.

The dynamical screening function can be used directly to evaluate carrier-carrier scattering and also describes how carrier-lattice scattering (including carrier-phonon and carrier-impurity scattering) is modified by screening. In polar semiconductors mutual screening of lattice and electronic modes leads to coupled plasmon–LO-phonon modes which within the RPA formalism can be described in terms of a coupling between the carrier and lattice screening functions.[9–11]

In this paper we study three different approximations to the full RPA expression for the dynamical screening function in detail: (i) the Lindhard zero-temperature RPA,[5,6] which should be valid at low temperatures and high carrier densities; (ii) a temperature-dependent two-pole approximation incorporating nondegenerate statistics,[12,13] which should be valid at low densities and a wide range of temperatures; and (iii) the plasmon-pole approximation.[2] Our primary goal is to establish the ranges of validity of the different models, in particular to establish the importance of temperature effects and to determine the density range above which the degeneracy of the sea of carriers becomes significant. We present results for differential scattering rates, mean free paths, and momentum-relaxation rates as functions of doping level, electron energy, and temperature for a hot electron traversing a heavily n-doped region in GaAs. Since this is a polar semiconductor we also consider the coupling of electrons to the LO phonons and present results for this system within the two-pole approximation. Some of the results for the two-pole approximation have been presented previously,[12,13] but here we have used a slightly different theoretical framework which enables us to evaluate differential scattering rates which are necessary for the eventual implementation of these scattering processes into a Monte Carlo transport simulation, which is one of the future aims of this work.

Our results are discussed in relation to experimental results on hot-electron transport[1,14,15] and compared to other theoretical results, including the recent finite-temperature RPA results of Hu and Das Sarma.[16]

In the next section we outline the general formalism and describe the three different models we have examined. In Sec. III we present a range of results that are discussed in Sec. IV. We finally summarize our conclusions in Sec. V.

II. THEORY

A. Formalism

In a homogeneous medium at temperature T with dielectric function $\epsilon(q,\omega;T)$ the doubly differential scattering rate for a particle with charge Ze, mass m^*, momentum $\hbar k$, and energy $E=\hbar^2k^2/(2m^*)$ derived from linear response theory is[4,17]

$$\frac{d^2\Gamma(\omega,q,E)}{d\omega dq}=\frac{2m^*Z^2e^2}{\hbar^2(4\pi\epsilon_0)}\frac{1}{\pi kq}\mathrm{Im}\left(\frac{-\epsilon_0}{\epsilon(q,\omega;T)}\right)\times\frac{1}{(\exp(\hbar\omega/k_BT)-1)}\Theta(q-q_-(\omega,E))\times\Theta(q_+(\omega,E)-q)\times[1-f(E-\hbar\omega-\mu)]\ , \tag{1}$$

where q and ω represent the momentum and energy transfer in the scattering process, respectively, and ϵ_0 is the vacuum permittivity. The factor $1-f$, where f is the Fermi function, takes into account the availability of final states for the scattered particle, assumed to be a fermion with chemical potential μ. The wave vectors q_- and q_+ are the minimum and maximum allowed momentum transfers determined by energy and momentum conservation for given values of k and ω:

$$q_-=\begin{cases}k-\sqrt{k^2+2m^*\omega/\hbar}, & \omega<0\\ -k+\sqrt{k^2+2m^*\omega/\hbar}, & \omega>0,\end{cases}$$

$$q_+=k+\sqrt{k^2+2m^*\omega/\hbar}\ . \tag{2}$$

Equation (1) shows that the scattering rates can be obtained directly if the dynamical response function $\epsilon(q,\omega;T)$ is known. Below we describe three different approximations to this response function.

The formulas above assume a parabolic band structure for the carriers. For polar semiconductors such as GaAs there are significant deviations from a parabolic band structure at higher energies. It is in principle simple to incorporate nonparabolicity for the hot carriers. However, our primary aim here is to make relative comparisons between different models. We are thus justified in neglecting this complication since the conclusions we draw from the results for parabolic bands can be assumed to hold also in the more general case with nonparabolic bands.

B. Model dielectric functions

1. Lindhard function

If the sea of carriers is assumed to be a free-electron gas present in a medium with a background dielectric constant ϵ_0^* and we set $T=0$, $\epsilon(q,\omega)\equiv\epsilon(q,\omega;T=0)$ corresponds to the well-known Lindhard dielectric function:[5,6]

$$\epsilon_L(q,\omega)=\epsilon_L^r(q,\omega)+i\epsilon_L^i(q,\omega), \tag{3}$$

$$\epsilon_L^r(q,\omega)/\epsilon_0=\frac{\epsilon_0^*}{\epsilon_0}+\frac{4}{\pi a_0q}\left\{\frac{1}{2}+\frac{1}{8z}\left[1-\left(z-\frac{x}{4z}\right)^2\right]\ln\left|\frac{z-x/4z+1}{z-x/4z-1}\right|+\frac{1}{8z}\left[1-\left(z+\frac{x}{4z}\right)^2\right]\ln\left|\frac{z+x/4z+1}{z+x/4z-1}\right|\right\}, \tag{4}$$

$$\epsilon_L^i(q,\omega)/\epsilon_0=\begin{cases}\pi x/(8z), & 0<x<4z(1-z)\\ \pi\left[1-\left(z-\frac{x}{4z}\right)^2\right]\Big/(8z), & 4z(z-1)<x<4z(z+1),\ x>4z(1-z)\\ 0\ \text{otherwise}\end{cases} \tag{5}$$

where a_0 is the Bohr radius, $x=\hbar\omega/E_F$, and $z=q/(2k_F)$, with E_F and k_F being the Fermi energy and wave vector, respectively.

Two distinct contributions to the scattering rates arise from the Lindhard dielectric function: single-particle excitations in the region limited by $4z(z-1)<x<4z(z+1)$ and plasmon excitations on the plasmon dispersion line defined by $\epsilon(q,\omega)=0$ outside the single-particle-excitation region.[6] Thus the dominant excitation at large q is single-particle excitation and at small q plasmon excitation.

2. Plasmon-pole approximation

In the plasmon-pole approximation the full range of excitations is replaced by a single mode. The dielectric function is written as[2]

$$\frac{\epsilon(q,\omega)}{\epsilon_0} = 1 - \frac{\omega_{pl}^2}{\omega^2 - (E_q/\hbar)^2} \tag{6}$$

where the plasmon frequency $\omega_{\rm pl}$ is defined by $\omega_{\rm pl}^2 = 4\pi ne^2/(m^*\epsilon_0^*)$ with n being the electron density and $E_q = \hbar^2 q^2/(2m^*)$. Thus the dispersion of the mode, which is given by the roots of the equation $\epsilon(q,\omega) = 0$, is $\omega(q) = \pm\sqrt{\omega_{\rm pl}^2 + (E_q/\hbar)^2}$ where the plus and minus signs represent absorption and emission, respectively. The plasmon-pole approximation, as described by Eq. (6), corresponds to the zero-temperature limit of the RPA for a nondegenerate electron gas.

3. Two-pole approximation

The two-pole approximation[12,18] to the temperature-dependent RPA provides a more detailed description of the excitations than the single plasmon-pole approximation since it takes into account the temperature dependence of the dielectric function. The dielectric function for a nondegenerate electron gas, i.e., a gas obeying Maxwell-Boltzman statistics, can be written as

$$\frac{\epsilon(q,\omega)}{\epsilon_0} = 1 + \left(\frac{k_D}{q}\right)^2 \left[\frac{Z\left(\xi - \frac{a}{2}\right) - Z\left(\xi + \frac{a}{2}\right)}{2a}\right] \tag{7}$$

with $\xi = \left[\sqrt{m^*/(2k_BT)}\right]\omega/q$, $a = \hbar q/\sqrt{2m^*k_BT}$, $k_D^2 = 4\pi ne^2/(\epsilon_0^* k_BT)$, and the function Z is the plasma dispersion function.[19] In the two-pole approximation Z is approximated by[18]

$$Z(s + i\delta) = \frac{i\sqrt{\pi} + (\pi - 2)s}{1 - i\sqrt{\pi}s - (\pi - 2)s^2} \quad . \tag{8}$$

Inserting Eq. (8) in Eq. (7) results in a dielectric function which is the ratio of two fourth-order polynomials in ω with coefficients which depend on q. The four (complex) roots of ϵ for a given q correspond to the emission and absorption of two branches of excitation modes. Although no formal distinction can be made between different types of excitations, the lowest-energy mode can be associated with single-particle excitations while the highest-energy mode accounts for plasmon excitation at low q and approaches the single particle branch at high q.

4. Coupled electron-phonon modes

A particular strength of the two-pole approximation is the ease with which the coupling of the electron system with other excitation modes can be incorporated. As an illustration of this we here present results for scattering off coupled electron-phonon modes. The dielectric function for the coupled system can be written:[13,20]

$$\epsilon(q,\omega) = \epsilon_e(q,\omega) + \epsilon_{\rm ph}(\omega) - \epsilon_0 \tag{9}$$

where ϵ_e is the dielectric function for the electronic system within the two-pole approximation as described above and $\epsilon_{\rm ph}$ is the dielectric function due to screening by optical phonons:

$$\epsilon_{\rm ph} = \epsilon_\infty^* + \frac{\epsilon_0^* - \epsilon_\infty^*}{1 - \omega^2/\omega_{\rm TO}^2} \tag{10}$$

where $\omega_{\rm TO}$ is the frequency of transverse-optical phonons and ϵ_∞^* is the high-frequency dielectric constant. The result for the coupled dielectric function is a ratio of two sixth-order polynomials in ω,[13] very similar to the ratio of fourth-order polynomials obtained for the electronic system without phonons (see above).

C. Calculated quantities

In Sec. III we present a number of results derived from the model dielectric functions described above. From the doubly differential scattering rate, defined by (1), we have evaluated the (singly) differential scattering rate

$$\frac{d\Gamma(\omega,E)}{d\omega} = \int_0^\infty dq \frac{d^2\Gamma(q,\omega,E)}{dqd\omega} \quad . \tag{11}$$

The total scattering rate is found as

$$\Gamma(E) = \int_{-\infty}^{\infty} d\omega \int_0^\infty dq \frac{d^2\Gamma(q,\omega,E)}{dqd\omega} \quad , \tag{12}$$

which is related to the mean free path λ as $\lambda(E) = (\hbar k/m^*)/\Gamma(E)$.

The mean free path describes the average distance traveled between scattering events, including those where the initial and final states have approximately the same momentum and energy. To obtain a more appropriate measure of the effect of scattering on carrier transport one needs a quantity which assigns more weight to those scattering events which change the momentum and/or energy of the carrier substantially. This is provided by the momentum relaxation length which is defined as $\lambda_k(E) = (\hbar k/m^*)/\Gamma_k(E)$ where the momentum relaxation rate Γ_k is given by

$$\begin{aligned}\Gamma_k(E) &= \int_{-\infty}^{\infty} d\omega \int_0^\infty dq \frac{d^2\Gamma(q,\omega,E)}{dqd\omega}\left(1 - \frac{k'}{k}\cos\theta\right) \\ &= \frac{1}{k^2}\int_{-\infty}^{\infty} d\omega \int_0^\infty dq \frac{d^2\Gamma(q,\omega,E)}{dqd\omega} \\ &\quad \times \left(q^2/2 - m^*\omega/\hbar\right) \quad .\end{aligned} \tag{13}$$

Here k and k' are the momenta before after scattering, respectively, and θ is the scattering angle. Additional information would be provided by the average energy loss/gain per collision which can easily be calculated from the differential scattering rates.

For the zero-temperature RPA the integrals can be split into plasmon and single-particle excitation contributions[6] which were evaluated numerically. In the case of the plasmon-pole approximation the ω integral has to be evaluated numerically.

For the two-pole approximation (with or without phonons) we evaluate all integrals numerically. This is in contrast to Refs. 12 and 13 where a temperature-dependent Green's-function approach was used to express the imaginary part of the self-energy, and hence the total

scattering rate, in terms of the dielectric function. This resulted in an expression with the ω integral, instead of being over the real axis, is a contour integral which, with a number of simplifications, could be evaluated analytically. However, numerical problems appear in the integrals for the "single-particle" branches for values of q where the real parts of the poles approach zero leading to divergent q integrals if the emission and absorption branches are evaluated separately. In order to steer clear of these problems and also to obtain an expression for $d^2\Gamma/dqd\omega$ we elected to use Eq. (1) instead of the self-energy expression of Ref. 12 and to evaluate both q and ω integrals numerically.

III. RESULTS

All results presented in this section correspond to n-doped GaAs. We have used the following parameters: $m^*=0.067m_0$, where m_0 is the free-electron mass, $\epsilon_0^*=12.53\epsilon_0$, $\epsilon_\infty^*=10.9\epsilon_0$, and $\hbar\omega_{TO}=33.6$ meV.

The mean free path for hot electrons in n-doped GaAs at low (zero or near-zero) temperature as function of the primary electron energy is shown in Fig. 1. The figure gives results for all three models for the dielectric response and for two different doping levels. The corresponding results for λ_k are shown in Fig. 2. The rapid

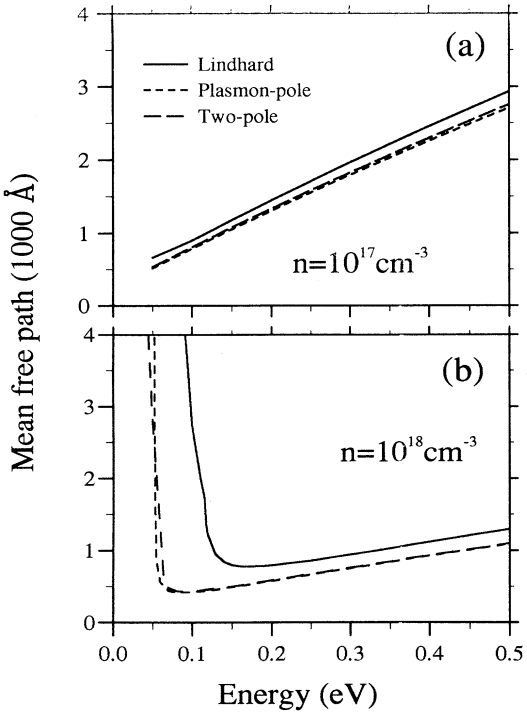

FIG. 1. The mean-free-path λ due to carrier-carrier scattering as a function of hot-electron energy in n-doped GaAs for doping levels 10^{17} and 10^{18} cm^{-3}. The long-dashed lines show the results from the two-pole approximation at temperature 10 K, the short-dashed lines the results from the plasmon-pole approximation at zero temperature, and the full lines the results from the zero-temperature RPA.

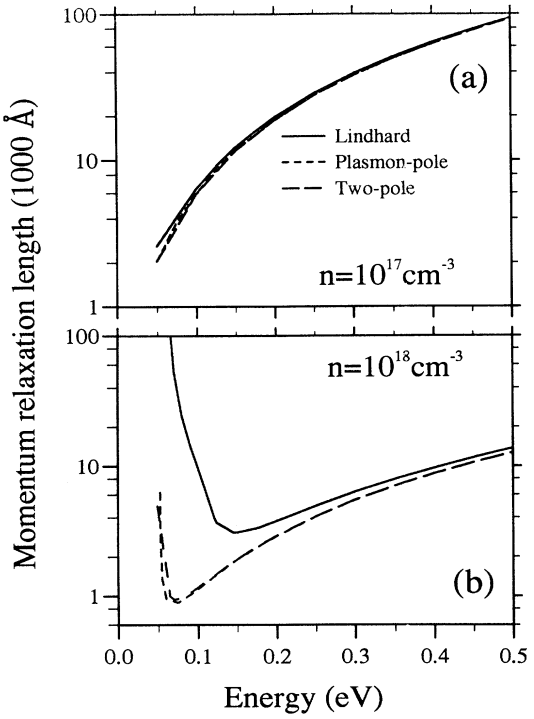

FIG. 2. The momentum relation length λ_k due to carrier-carrier scattering as a function of electron energy for three different doping levels. Notation is the same as in Fig. 1. Note the logarithmic abscissas.

decrease in both λ_k and λ at low energy for $n = 10^{18}$ cm^{-3} signifies the onset of plasmon emission (a similar behavior occurs for $n = 10^{17}$ cm^{-3} below the energy region for which data are shown in the figures). It is apparent from Figs. 1 and 2 that the two-pole approximation and the full zero-temperature RPA (Lindhard function) agree well when the primary energy of the hot carrier is much greater than the Fermi energy, but the neglect of degeneracy in the two-pole approximation makes it inaccurate for energies comparable to the Fermi energy. For a typical hot-electron energy, e.g., in the base of a hot-electron transistor,[1,15] of 0.25 eV, this means that for doping densities near 10^{18} cm^{-3} and above the two-pole approximation becomes inaccurate while for lower densities the neglect of degeneracy is justified.

The figures show that below about 0.3 eV both mean free paths and momentum-relaxation lengths are of the order of 1000 Å. At higher energies both λ_k and λ increase with λ_k increasing more rapidly with E. The reason for this is that as the carrier energy is increased the scattering becomes increasingly forward peaked, i.e., low-q scattering events, which contribute only weakly to the momentum-relaxation rate, dominate.

At low energies, below 0.3 eV, carrier-carrier scattering is one of the dominant scattering mechanisms in heavily doped GaAs along with polar optical-phonon scattering and impurity scattering. The results thus imply that hot-electron path lengths of the order of 1000 Å can be obtained at low temperatures, a fact confirmed by

experiments on hot-electron transistors.[1,14,15] At higher carrier energies other scattering processes, in particular intervally scattering, prevent the very long path lengths calculated when considering only carrier-carrier and (intravalley) phonon scattering from being realized experimentally.

Figures 3 and 4 demonstrate the temperature dependence of the mean free paths and momentum-relaxation lengths, respectively, calculated within the two-pole and plasmon-pole approximations. It is clear from Figs. 3 and 4 that the temperature dependence of the scattering is substantial for n less than 10^{18} cm^{-3}. It is thus important to incorporate the temperature effects when modelling hot-electron transport at nonzero temperatures even for moderately high doping densities. In contrast, for $n = 10^{18}$ and above, the full zero-temperature RPA describes the scattering even at nonzero temperatures reasonably accurately.

Figures 1 and 2 demonstrate that the two-pole and plasmon-pole approximations agree well at low temperatures. However, the temperature dependence of the scattering in the plasmon-pole approximation is much stronger than in the two-pole approximation as is demonstrated by Figs. 3 and 4. This is to be expected since the only temperature dependence included in the plasmon-pole approximation is the Bose factor $[1-\exp(\hbar\omega/kT)]^{-1}$ in Eq. (1) while the temperature dependence of the screening, i.e., $\epsilon(q,\omega)$, is ignored, unlike in the two-pole approximation. The results show that the true path lengths at finite temperatures are likely to be significantly *longer* than predicted by the simple plasmon-pole approximation.

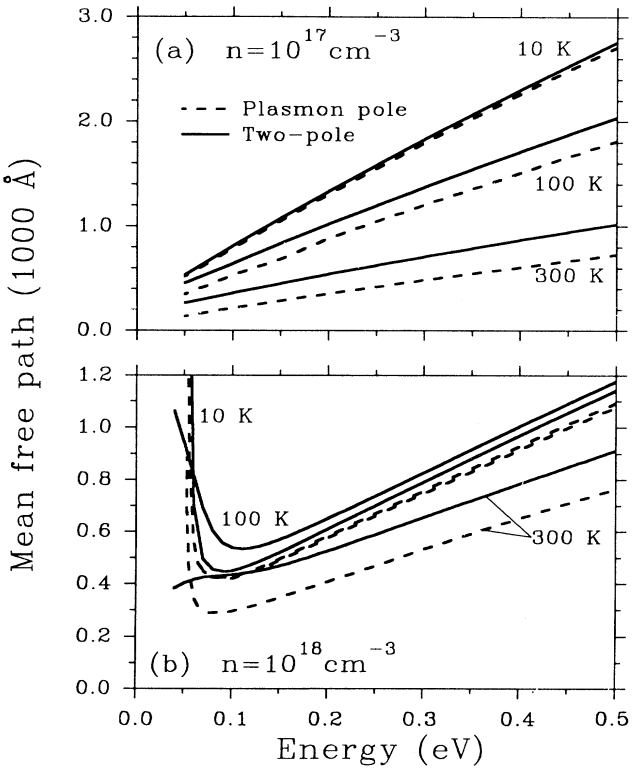

FIG. 3. The mean free paths of an electron in n-doped GaAs at three different temperatures at doping levels 10^{17} and 10^{18} cm^{-3}. Full and dashed curves were obtained with the two-pole and plasmon-pole approximations, respectively.

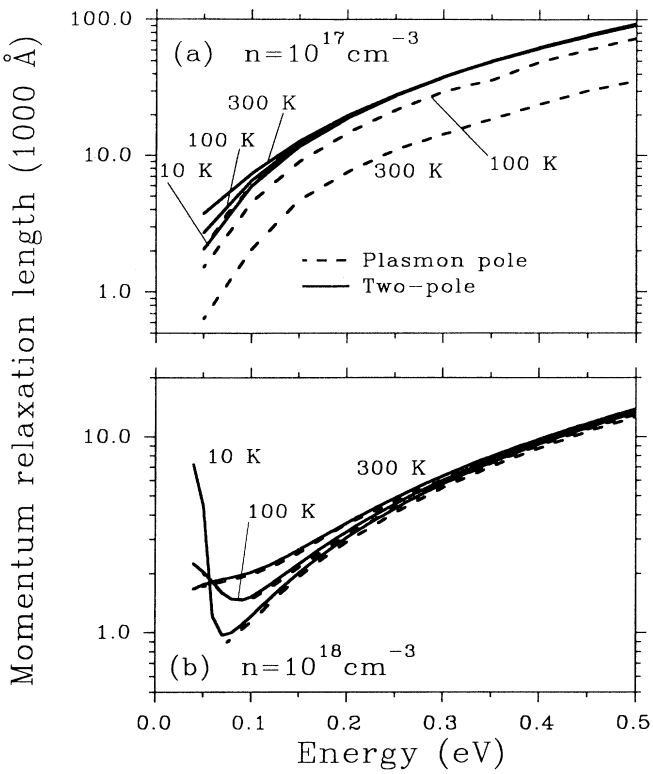

FIG. 4. The momentum-relaxation lengths of an electron in n-doped GaAs at three different temperatures at doping levels 10^{17} and 10^{18} cm^{-3}. Full and dashed curves were obtained with the two-pole and plasmon-pole approximations, respectively. Note the logarithmic abscissas.

A more detailed comparison between the two-pole and Lindhard approximations is provided by Fig. 5, which shows the differential scattering rate for $n = 10^{17}$ cm^{-3} and E=0.3 eV at low temperature. The most prominent feature is the plasmon emission, which is represented by a sharp peak around -50 meV in all three models. However, the total contributions from plasmons and single-particle scattering in the zero-temperature RPA are comparable in magnitude. The two approximations are seen to agree well at all ω, including the regions where the scattering is dominated by single-particle excitations, but only the two-pole approximation describes the broadening of the onset of the plasmon excitations due to plasmon damping.

The temperature dependence of the differential scattering rate within the two-pole approximation is given in Fig. 6 for n=10^{17} cm^{-3}. The figure shows that as the temperature is raised, absorption processes become increasingly important, the plasmon emission and absorption lines are broadened and the scattering off low-energy

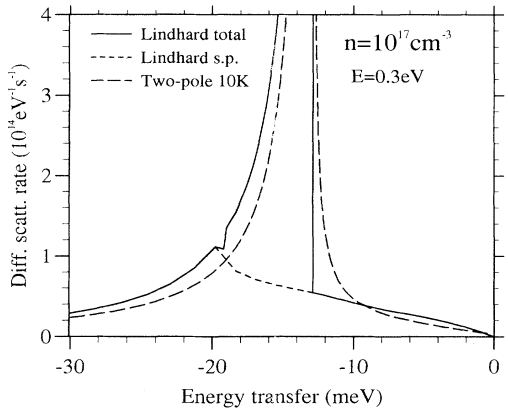

FIG. 5. The differential scattering rate as a function of energy transfer $\hbar\omega$ for $n=10^{17}$ cm^{-3} and $E=0.3$ eV. The full curve shows the two-pole approximation result for temperature 10 K and the dot-dashed curve the zero-temperature RPA (Lindhard) result. The contributions from single-particle excitations within the zero-temperature RPA is shown separately as the short-dashed line. The plasmon peak near -50 meV reaches in both cases values of $d\Gamma/d\omega$ above 50×10^{14} eV^{-1}s^{-1}.

single-particle excitations increases. The latter two features are not included in the simpler plasmon-pole approximation.

We do not present results for the average energy loss/gain per collision. However, it is evident from Figs. 5 and 6 that energy loss and gain processes are dominated by the plasmon peaks in the differential scattering rate, which implies that the average energy loss or gain per collision will be close to the plasmon energy.

Finally we show in Fig. 7 mean free paths for scattering off a coupled system of phonons and electrons within the two-pole approximation, see Sec. II B 4, for $n=5\times10^{17}$ cm^{-3} where the coupling between optical phonons and plasmons is strong. The figure demonstrates the importance of the temperature dependence also when the electron system is coupled to phonons.

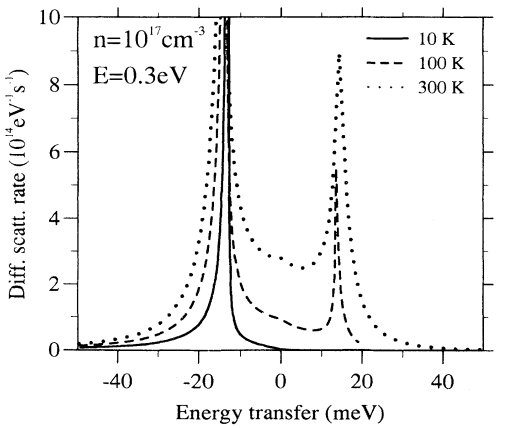

FIG. 6. The differential scattering rate as a function of energy transfer $\hbar\omega$ for $n=10^{17}$ cm^{-3}, $E=0.3$ eV, and three different temperatures as indicated in the figure. All results were obtained with the two-pole approximation.

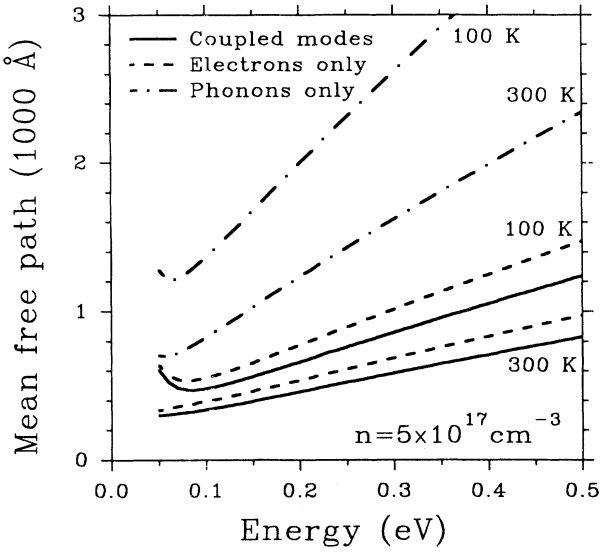

FIG. 7. The mean free path for hot electrons in a system of coupled phonons and electrons with density $n=5\times10^{17}$ cm^{-3} at temperatures 100 and 300 K calculated using the two-pole approximation for the electronic part of the dielectric function (full lines). The mean free paths for systems of phonons and electrons only are shown as the dot-dashed and dashed lines, respectively, the latter calculated with the two-pole approximation.

IV. DISCUSSION

An important conclusion which can be drawn from the results in Sec. III is that the zero-temperature RPA (Lindhard dielectric function) and the two-pole approximation together provide an adequate description of carrier-carrier scattering over a wide range of doping densities and temperatures. At high densities the degeneracy of the electron system is important, but temperature effects are small, which means that the zero-temperature RPA provide an accurate description at these densities. At low densities temperature effects are more pronounced, but the use of Maxwell-Boltzmann statistics, i.e., assuming a nondegenerate electron gas, is justified for typical hot-electron energies in devices.

In n-type GaAs the crossover between the validity of the two models lies for typical hot-electron energies around 10^{18} cm^{-3}. This crossover density will depend on the effective mass of the carriers. For higher masses the crossover density will be higher and the two-pole approximation will be valid at substantially higher densities in Si hot-electron transistors and in p-doped bases of heterojunction bipolar transistors[1] where the hole masses are larger than the electron masses in GaAs.

Several authors have compared low-temperature results for hot-electron spectrometers or experiments on hot electrons in optically excited semiconductors with

theories based on the Lindhard dielectric function coupled to LO phonons.[14,15,21] In all cases the agreement was found to be good. At higher temperatures increased scattering reduces the hot-electron path lengths and the performance of hot-electron transistors is degraded. However, our results, in particular Figs. 3 and 4, show that the reduction in path length is not as severe as predicted by using the plasmon-pole approximation to estimate carrier-carrier scattering. Thus, for hot-carrier devices operating at room temperature it is important to include an accurate description of carrier-carrier scattering, incorporating temperature effects properly, in modelling of these devices, e.g., by Monte Carlo simulation.

In addition to the results presented in the figures we performed calculations at the same electron densities as Hu and Das Sarma,[16] who used the temperature-dependent degenerate RPA to calculate scattering rates for hot electrons in n-GaAs. We found, as expected, that the two calculations agree well (within 10%) when the hot-electron energy is substantially larger than the Fermi energy (in practice larger than five times E_F).

We have in this paper restricted ourselves to discussing the scattering of a single hot electron off a sea of conduction electrons in thermal equilibrium appropriate for hot-electron transistors. However, the present models, in particular the two-pole approximation, should also be valuable in modeling the contribution to the screening from electrons and holes in optically excited semiconductors, although in these cases complications arise because carriers are scattered by both electrons and holes in electron-hole plasmas[22–24] and because the scatterers (electrons, holes, phonons) are not necessarily in thermal equilibrium.[25,26] The most immediate extension of our theory will be the calculation of scattering of carriers by coupled light- and heavy-hole plasmas including coupling with LO phonons.[27]

V. CONCLUSION

We have discussed a number of different descriptions of the scattering of hot carriers off high densities of carriers in semiconductors and examined the range of validity for each model. In particular, we have shown that the two-pole approximation to the temperature-dependent RPA (Refs. 12 and 13) is expected to be valid for the typical ranges of doping densities, temperatures, and hot-electron energies.

We have also emphasized the importance of including the temperature dependence of the dielectric response and, in particular, shown that the two-pole approximation provides a convenient way of including this effect in practical calculations.

ACKNOWLEDGMENTS

We would like to thank David Herbert (Defence Research Agency, Malvern) and David Neilson (University of New South Wales) for useful discussions and Robert Smith (Sharp Laboratories of Europe Ltd.) for computational assistance.

[1] J.R. Hayes and A.F.J. Levi, IEEE J. Quantum Electron. **QE-22**, 1744 (1986).
[2] D.C. Herbert, Semicond. Sci. Technol. **7**, 44 (1992).
[3] G.D. Mahan, *Many-Particle Physics* (Plenum, New York, 1981).
[4] A.L. Fetter and J.D. Walecka, *Quantum Theory of Many-particle Systems* (McGraw-Hill, New York, 1971).
[5] J. Lindhard, Kong. Dansk. Vidensk. Selsk. Mat.-Fys. Medd. **28**, 1 (1954).
[6] C.J. Tung and R.H. Ritchie, Phys. Rev. B **16**, 4302 (1977).
[7] D. Bohm and D. Pines, Phys. Rev. **92**, 609 (1953).
[8] P. Lugli and D.K. Ferry, Physica B **117**, 251 (1983); **129**, 532 (1985).
[9] S.E. Kumekov and V.I. Perel', Fiz. Tekh. Poluprovodn. **16**, 2001 [Sov. Phys. Semicond. **16**, 1291 (1982)].
[10] M.E. Kim, A. Das, and S.D. Senturia, Phys. Rev. B **18**, 6890 (1978).
[11] D. Neilson, J. Szymanski, and De-Xin Lu, J. Phys. (Paris) Colloq. **48**, C5-263 (1987).
[12] J.M. Rorison and D.C. Herbert, J. Phys. C **19**, 3991 (1986).
[13] J.M. Rorison and D.C. Herbert, J. Phys. C **19**, 6357 (1986).
[14] A.F.J. Levi, J.R. Hayes, P.M. Platzman, and W. Weigmann, Phys. Rev. Lett. **55**, 2071 (1985).
[15] A.P. Long, P.H. Beton, and M.J. Kelly, Semicond. Sci. Technol. **1**, 63 (1986).
[16] Ben Yu-Kuang Hu and S. Das Sarma, Semicond. Sci. Technol. **7**, B305 (1992).
[17] P.M. Platzman and P.A. Wolff, *Solid State Physics, Supplement 13* (Academic Press, New York, 1973).
[18] D. Lowe and J.R. Barker, J. Phys. C **18**, 2507 (1985).
[19] B.D. Fried and S.D. Conte, *The Plasma Dispersion Function* (Academic, London, 1961).
[20] B.B. Varga, Phys. Rev. **137**, A1896 (1965).
[21] C.L. Peterson and S.A. Lyon, Phys. Rev. Lett. **65**, 760 (1990).
[22] J.A. Kash, Phys. Rev. B **40**, 3455 (1989).
[23] J.F. Young, N.L. Henry and P.J. Kelly, Solid-State Electron. **32**, 1567 (1989); J.F. Young, P.J. Kelly, N.L. Henry, and M.W.C. Dharma-wardana, Solid State Commun. **78**, 343 (1991).
[24] K. Leo and J.H. Collet, Phys. Rev. B **44**, 5535 (1991).
[25] J.K. Jain, R. Jalabert, and S. Das Sarma, Phys. Rev. Lett. **60**, 353 (1988); S. Das Sarma, J.K. Jain, and R. Jalabert, Phys. Rev. B **41**, 3561 (1990).
[26] M.W.C. Dharma-wardana, Phys. Rev. Lett. **66**, 197 (1991); S. Das Sarma and V. Korenman, *ibid.* **67**, 2916 (1991); M.W.C. Dharma-wardana, *ibid.* **66**, 2917 (1991).
[27] V. Narayan, J.M. Rorison, and K.O. Jensen (unpublished).